Volume Title
ASP Conference Series, Vol. **Volume Number**
Author

Understanding the differences in 3 consecutive large flares

Lucas Tarr[1] and Dana Longcope,[1]

[1]*Department of Physics, Montana State University, Bozeman, Montana 59717*

Abstract. The active region NOAA 11158 produced three large flares over a 31 hour interval centered on 14 Feb. 2011. The flare ribbons observed in 1600Å AIA images reveal very different characters between the three. We use a model of the coronal magnetic field topology and its evolution to explain the differences in structures and energies of these three flares.

According to the prevailing picture, coronal magnetic energy is stored slowly through stressing from below (the photosphere) and released rapidly by reconnection, producing flares. A single active region (AR) typically undergoes repeated flares presumably separated by periods of energy replenishment. Certain cases, called *homologous flares*, appear to release similar amounts of energy in similar ways each time (Sui et al. 2004). The process of release, believed to be magnetic reconnection, is complex enough that one expects such replication to be the exception rather than the rule. Here we analyze three successive flares which evidently each result from a different reconnection processes.

Steady energy build–up occurs in AR NOAA 11158,[1] visible on the disk between 10 Feb 2011 and 19 Feb 2011. This AR hosted three major flares as it passed the central meridian: an M6.6 flare on 13 Feb at 17:30, an M2.2 flare on 14 Feb at 17:20, and an X2.2 flare on 15 Feb at 01:45. We model the topology and energy build-up using a sequence of line-of-sight magnetograms from SDO/HMI (Schou et al. 2011; Wachter et al. 2011) at a cadence of 24 minutes, beginning 11 Feb at 8:10. We apply the MCC method of Tarr & Longcope (2012) to partition the magnetogram flux into sequence of unipolar, photopsheric regions. These regions form a quadrupole whose flux increases, and whose elements move relative to one another. Both processes store energy in the coronal field according to the Minimum Current Corona model (MCC, Longcope 2001; Longcope & Klapper 2002; Longcope & Magara 2004; Kazachenko et al. 2010, 2011; Tarr & Longcope 2012). It is this energy which is released during the three flares.

The topology of the corona field is summarized by its so–called skeleton (Priest et al. 1997) consisting of the spines, fan surfaces and their intersections along separators. These features are plotted in Figure 1 (spines as solid lines, separators as dashed lines) atop representative 1600 Å images (from SDO/AIA, Lemen et al. 2011) from each of the flares. Flare ribbons appear clearly in this bandpass, revealing the field lines being reconnected to release the stored energy. Ribbons tend to follow the spine lines bounding the flux domains involved in the reconnection (Des Jardins et al. 2009; Kazachenko et al. 2010, 2011). Since the skeleton is computed using a potential field,

[1]SOL2011-02-13T17:30:00L034C110

extrapolated from point sources, the spines do not match the ribbon locations precisely, but the resemblance is generally clear enough for the reconnection scenario to be inferred.

This sequence of images show that each flare reconnects a different set of field lines, thereby releasing energy stored in different portions of the coronal field. The first flare in the sequence (M6.6 in Figure 1a) has a single strong ribbon which we believe to be a combination of both the traditional ribbons: it lies in a region of negative flux, along spines connecting poles N2/N26, and positive flux where a spine would connect P3/P37.[2] These spines are associated with domains near the center and to the Northwest of the active region. The implication is that field lines initially connecting P3–N2 and P37–N26 are being broken to connect P37–N2 and P3–N26 and thereby lowering the coronal field energy.

The second flare (M2.2 flare in Figure 1b) occurs 24 hours later, with ribbons in a different portion of the AR. This is the only one with notable ejection — even evident in 1600 Å. The ejection and the ribbons occur near a recently emerged bipole, P52/N56, in the Eastern portion of the AR. The bipole emerges as a twisted flux rope, and its emergence generates a pitchfork bifurcation(Brown & Priest 1999) of a null between N2 and N25, creating a coronal null in the process. The ribbons in this flare are fainter, and difficult to differentiate from ejecta. They principally follow spines in the Southwest associated with the emerging bipole: the P61/P64/P59 in the positive region and N56/N1/N61. The spine lines of the coronal null appear to act as a bridge, allowing the Southwest reconnection to activate domains associated with spines linking N2/N35 and P3/P64, near the AR center. The lack of spines associated with ribbons around the twisted flux rope indicates the limitations of potential field extrapolations for modeling such systems.

The final flare (X2.2 in Figure 1c) is the largest and most extensive of the three. Its ribbons follow spines between P88/P39, P1/P39, P3/P39, our assumed realistic spine between P3/P64, P64/P52, N2/N26, N25/N56, and N25/N29, spanning the entire AR. The strongest of these suggest significant reconnection producing new field lines connecting P64–N2 and P59–N26, among others. These field lines are in the center of the AR, but link polarities which had emerged in separate bipoles. Since neither of the previous flares achieved this reconnection, its energy had remained untapped to be released in this later, larger flare.

Acknowledgments. Our 2011 REU student Megan Millhouse generated the mask structures for the magnetogram data series. This work was supported by NASA LWS.

References

Brown, D. S., & Priest, E. R. 1999, Proc. R. Soc. Lond. A, 455, 3931

Des Jardins, A., Canfield, R., Longcope, D., Fordyce, C., & Waitukaitis, S. 2009, ApJ, 693, 1628

Kazachenko, M. D., Canfield, R. C., Longcope, D. W., & Qiu, J. 2010, ApJ, 722, 1539

— 2011, Solar Phys.(submitted). 1104.3593

Lemen, J. R., Title, A. M., Akin, D. J., Boerner, P. F., Chou, C., Drake, J. F., Duncan, D. W., Edwards, C. G., Friedlaender, F. M., Heyman, G. F., Hurlburt, N. E., Katz, N. L., Kushner, G. D., Levay, M., Lindgren, R. W., Mathur, D. P., McFeaters, E. L., Mitchell, S., Rehse,

[2]MCT splits the spine line between P3 and P37 into P3/P59/P37.

R. A., Schrijver, C. J., Springer, L. A., Stern, R. A., Tarbell, T. D., Wuelser, J.-P., Wolfson, C. J., Yanari, C., Bookbinder, J. A., Cheimets, P. N., Caldwell, D., Deluca, E. E., Gates, R., Golub, L., Park, S., Podgorski, W. A., Bush, R. I., Scherrer, P. H., Gummin, M. A., Smith, P., Auker, G., Jerram, P., Pool, P., Soufli, R., Windt, D. L., Beardsley, S., Clapp, M., Lang, J., & Waltham, N. 2011, Solar Phys., 172

Longcope, D., & Klapper, I. 2002, ApJ, 579, 468

Longcope, D., & Magara, T. 2004, ApJ, 608, 1106

Longcope, D. W. 2001, Physics of Plasmas, 8, 5277

Priest, E. R., Bungey, T. N., & Titov, V. S. 1997, Geophys. Astrophys. Fluid Dynamics, 84, 127

Schou, J., Scherrer, P. H., Bush, R. I., Wachter, R., Couvidat, S., Rabello-Soares, M. C., Liu, Y., Hoeksema, J. T., Bogart, R. S., Duvall, J. T. L., Miles, J. W., Title, A. M., Shine, R. A., Tarbell, T. D., Allard, B. A., Wolfson, C. J., Tomczyk, S., Norton, A. A., Elmore, D. F., & Borrero, J. M. 2011, Solar Phys.

Sui, L., Holman, G. D., & Dennis, B. R. 2004, ApJ, 612, 546

Tarr, L. A., & Longcope, D. W. 2012, ApJ

Wachter, R., Schou, J., Rabello-Soares, M. C., Miles, J. W., Duvall, T. L., & Bush, R. I. 2011, Solar Phys., 100

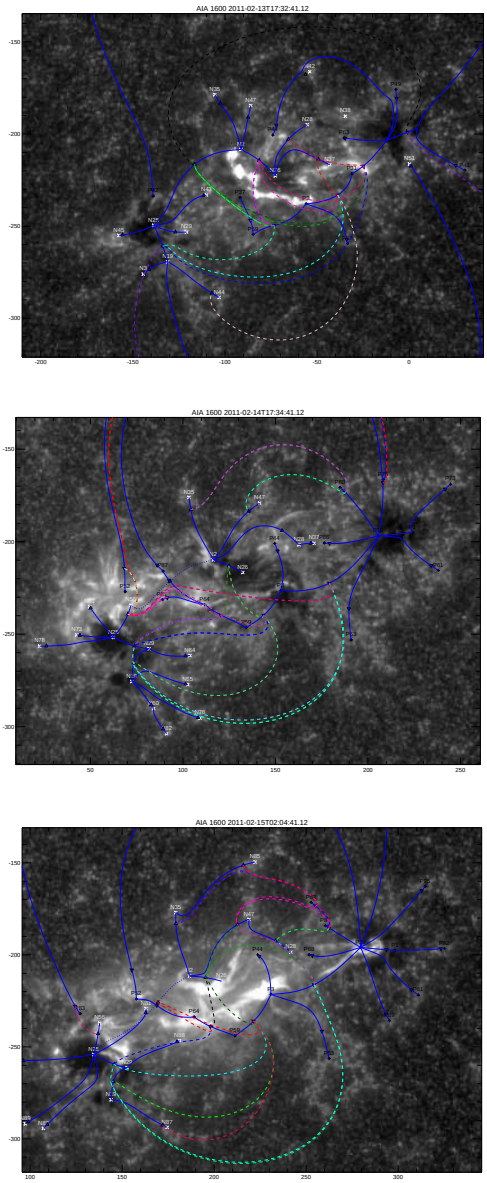

Figure 1. Magnetic topology overlaying AIA 1600Åimages during the (a) M6.6, (b) M2.2, and (c) X2.2 flares. Pluses and crosses denote the flux–weighted centroids of positive and negative magnetic flux regions, respectively. Triangles show the locations of null points in the potential field extrapolation, and blue solid lines the spine field lines from each null point. Dashed lines are the separators. The dotted line is the spine line of the coronal null, located roughly 3Mm and 10Mm above the photosphere in figures (b) and (c), respectively.